



Published in final edited form as:

Neuron. 2015 February 18; 85(4): 804–818. doi:10.1016/j.neuron.2014.12.061.

Light and hydrogen peroxide inhibit *C. elegans* feeding through gustatory receptor orthologs and pharyngeal neurons

Nikhil Bhatla^{1,2} and H. Robert Horvitz^{1,*}

¹Howard Hughes Medical Institute and Department of Biology, Massachusetts Institute of Technology, 77 Massachusetts Avenue, Cambridge, MA, USA 02139

²Department of Brain and Cognitive Sciences, Massachusetts Institute of Technology, 77 Massachusetts Avenue, Cambridge, MA, USA 02139

SUMMARY

While gustatory sensing of the five primary flavors (sweet, salty, sour, bitter, and savory) has been extensively studied, pathways that detect non-canonical taste stimuli remain relatively unexplored. In particular, while reactive oxygen species cause generalized damage to biological systems, no gustatory mechanism to prevent ingestion of such material has been identified in any organism. We observed that light inhibits *C. elegans* feeding and used light as a tool to uncover molecular and neural mechanisms for gustation. Light can generate hydrogen peroxide, and we discovered that hydrogen peroxide similarly inhibits feeding. The gustatory receptor family members LITE-1 and GUR-3 are required for the inhibition of feeding by light and hydrogen peroxide. The I2 pharyngeal neurons increase calcium in response to light and hydrogen peroxide, and these responses require GUR-3 and a conserved antioxidant enzyme peroxiredoxin PRDX-2. Our results demonstrate a gustatory mechanism that mediates the detection and blocks ingestion of a non-canonical taste stimulus, hydrogen peroxide.

INTRODUCTION

Animals are heterotrophs that rely on the ingestion of other organisms as food to survive and flourish. When selecting an object to eat, an animal must assess whether that object is likely to be nutritious and unlikely to be toxic. An animal safely samples a prospective food source by using its chemoreceptive senses to smell and taste the object before ingesting it. Both vertebrates, such as humans and mice, and invertebrates, such as the fruit fly *Drosophila melanogaster*, have taste receptors for detecting sugars, salts, amino acids and nucleotides

© 2014 Elsevier Inc. All rights reserved.

* Correspondence to horvitz@mit.edu.

Publisher's Disclaimer: This is a PDF file of an unedited manuscript that has been accepted for publication. As a service to our customers we are providing this early version of the manuscript. The manuscript will undergo copyediting, typesetting, and review of the resulting proof before it is published in its final citable form. Please note that during the production process errors may be discovered which could affect the content, and all legal disclaimers that apply to the journal pertain.

AUTHOR CONTRIBUTIONS

N.B. designed and conducted experiments and analyzed data; H.R.H. designed experiments and supervised; N.B. and H.R.H. wrote the manuscript. All software developed during the course of these experiments is available from WormWeb.org (<http://www.wormweb.org>).

(which to humans have a savory or umami flavor), acidic pH (which tastes sour), and a large variety of compounds that activate bitter receptors (Liman et al., 2014). Sweet, salty, and savory flavors indicate the presence of nutritious compounds and generally lead to ingestion. By contrast, bitter flavors can indicate the presence of toxins (Sandell and Breslin, 2006), and sour flavors can indicate the presence of damaging acids and pathogenic contaminants such as those that occur in spoiled food (Lindemann, 2001). Both bitter and sour flavors generally block ingestion to prevent damage and sickness caused by poisons and pathogens.

Taste has been studied extensively in the context of the five primary flavors, and molecular and cellular components for the gustatory detection of non-canonical taste stimuli, such as carbonation (CO₂), water, glycerol, and fatty acids, have also been identified (Fischler et al., 2007; Chandrashekar et al., 2009; Cameron et al., 2010; Chen et al., 2010; Wisotsky et al., 2011; Cartoni et al., 2010; Masek and Keene, 2013). However, little is known about how reactive oxygen species, such as hydrogen peroxide (H₂O₂), affect gustatory sensation. When ingested, hydrogen peroxide can cause oxidative stress and other deleterious effects, as demonstrated in humans (Cina et al., 1994). Microorganisms adapt to oxidative stress by detecting hydrogen peroxide via direct protein oxidation, which triggers a transcriptional response (Storz et al., 1990; Delaunay et al., 2002). More generally, the functions of many proteins can be modified as a result of oxidation by hydrogen peroxide (Veal et al., 2007). However, gustatory sensation of hydrogen peroxide has not been described for any animal.

The nematode *Caenorhabditis elegans* is an excellent animal to use for studies of taste mechanisms because of its genetic tractability and because feeding is easily scored and known to be modulated by food and other gustatory stimuli. Feeding is observed as “pumps” of the pharyngeal grinder, which are scored using a dissecting microscope. Pumping rate is increased by the presence of bacterial food (Horvitz et al., 1982) and bacterial products such as diacetyl (Li et al., 2012), while the bitter compound quinine reduces ingestion by decreasing pumping (Li et al., 2012). Beyond these examples, however, the feeding effects of other gustatory stimuli, including hydrogen peroxide, remain relatively unexplored in the worm.

By analyzing the behavioral effects of light on *C. elegans*, we discovered that *C. elegans* pumping is inhibited by light and that this inhibition is mediated by gustatory receptor (GR) orthologs. GRs are a molecular class of taste receptors identified in insects, and the *C. elegans* genome contains genes orthologous to this class (Robertson et al., 2003). Ultraviolet (UV) light causes locomotory avoidance by both *C. elegans* and the fruit fly *Drosophila melanogaster*, and this avoidance requires LITE-1 and GR28B, respectively, both members of the gustatory receptor family (Edwards et al., 2008; Ward et al., 2008; Liu et al., 2010; Xiang et al., 2010). As we explored the behavioral effects of light on *C. elegans*, we observed that light also inhibits feeding. We used the feeding response to light as a tool to investigate mechanisms that control feeding behavior and identified a novel gustatory receptor ortholog, GUR-3, and pharyngeal neurons, the I2s, that function for the detection of hydrogen peroxide and the inhibition of feeding that is caused by hydrogen peroxide.

RESULTS

Light inhibits feeding

C. elegans feeding can be observed by scoring pharyngeal pumping. Each pump involves a posterior-directed contraction of the grinder followed by an anterior-directed relaxation (Figure 1A). At room temperature (22-23 °C) and in the presence of bacterial food, worms pump between 4 and 5 times per second (4-5 Hz). We scored feeding in real-time by eye. We found that exposure to violet light severely disrupted this feeding rhythm (Figures 1B and 1C; Movie S1) and confirmed this finding by analyzing high-frame-rate videos (86 fps, Figure S1A). We used 436 nm violet light (13 mW/mm²) as the light stimulus, unless stated otherwise. The pumping response can be divided into four phases. First, pumping immediately stops in response to light (the “acute” response, 0-5 s after light onset). Second, pumping rate increases, plateaus, then decreases while light is maintained (the “burst” response, 5-20 s after light onset). Third, pumping remains suppressed while light is maintained (the “sustained” response, 20-60 s after light onset). Fourth, pumping slowly recovers after light is removed (the “recovery” response, 0-10 s after light removal) (Figures 1C and S2). In the experiments that follow, light was provided for 10 s, and we focused on analyzing the acute response.

To determine the spectral sensitivity of the pumping response to light, we varied both the wavelength and power of light. The pumping response was elicited most strongly by the shortest wavelength of light that we could deliver through our microscope (350 nm UVA, 0.2 mW/mm²), and can be elicited by higher power light of longer wavelengths (500 nm green, 6 mW/mm²) (Figures 1D-1H). Similar spectral and power sensitivity has been reported for the locomotory avoidance of *C. elegans* to light (Edwards et al., 2008; Ward et al., 2008).

To determine if the behavioral responses to light might be caused by heat, we first measured the temperature change at the agar surface after exposure to light for 10 s and found that temperature increased 1-2.1 °C. Next, we increased the temperature of the worm and found that a 7 °C increase did not evoke feeding inhibition or avoidance (Figure S3A). A 12 °C increase did evoke feeding inhibition and avoidance, but this response was independent of the gustatory receptors we found to function in behavioral responses to light (see below) (Figure S3B). We conclude that the response to light is unlikely to be a response to temperature increase.

Gustatory receptor orthologs *lite-1* and *gur-3* are required for feeding inhibition by light

Since the locomotory avoidance caused by UV light requires the gustatory receptor ortholog LITE-1 (Edwards et al., 2008; Liu et al., 2010), we tested whether LITE-1 was also involved in the feeding response to light. *lite-1(ce314)* mutants exhibited defects in the acute and recovery responses to light (Figures 2A, 2D-2F). In addition, we tested genes known to function downstream of *lite-1* in the ASJ sensory neurons (Ward et al., 2008; Liu et al., 2010). Mutants of the G proteins *goa-1(n1134)* and *gpa-3(pk35)*, guanylyl cyclases *daf-11(m47)* and *odr-1(n1936)*, phosphodiesterases *pde-1,2,3,5*, and cGMP-gated ion channels *tax-2(p671)* and *tax-4(p678)* did not have a defective acute response to light

(Figure S4). These results indicate that *lite-1* functions in the pumping response to light through genes other than those required for the response of the ASJ neurons to light.

To determine where *lite-1* is expressed and identify likely sites of *lite-1* function, we generated and examined worms carrying one of four transgenes derived from the wild-type *lite-1* locus: a genomic fragment (*lite-1* genomic), a transcriptional fusion (*lite-1_{prom}::gfp*), a C-terminal translational fusion (*lite-1_{prom}::lite-1::gfp*), and an N-terminal translational fusion (*lite-1_{prom}::gfp::lite-1*) (Figure S5A). Transgenes containing the *lite-1* genomic locus as well as the C-terminal and N-terminal fusions rescued the pumping-inhibition and light-avoidance phenotypes of the *lite-1* mutant (Figures S5B-S5H), suggesting that *lite-1* normally functions in at least some of the cells in which GFP was expressed. We observed such GFP expression in a total of 29 cells: pharyngeal neurons M1, M4, M5 and MI; non-pharyngeal neurons ASK, ADL, ASI, ASH, AVG, AVB, RIM, ADF, PHA, PHB and PVT; and non-neuronal cells Hyp3 (hypoderm), AMso (amphid socket cells) and PHso (phasmid socket cells) (Figure S5I-S5K). AVB was observed only with the C-terminal fusion transgene, and RIM and ADF were observed only with the transcriptional fusion transgene. *lite-1* expression in AVG and PVT was previously reported (Edwards et al., 2008).

To identify genes responsible for the response that remained in the *lite-1* mutants, we tested other members of the *C. elegans* family of gustatory receptor orthologs (Figure S6A). While mutants of *egl-47(n1081)*, *egl-47(ok677)* and *gur-4(ok672)* had a normal light-induced pumping response (Figures S6B-S6D), mutants of *gur-3(ok2245)*, the closest *lite-1* paralog (Figure S6E), exhibited a defect in the acute pumping response (Figures 2B, 2D-2F). The *ok2245* mutation deletes 1,208 bases, inserts two bases immediately after the first exon and is predicted to result in a premature stop codon. Another *gur-3* deletion mutant, *ok2246*, also exhibited a similar defect in its acute pumping response to light (Figure S6F). Strikingly, *lite-1 gur-3* double mutants were severely defective in the pumping response to light (Figures 2C-2F), indicating that these two gustatory receptor orthologs function together in the feeding response to light.

***gur-3* functions in the I2 pharyngeal neurons for light-induced inhibition of feeding**

To identify candidate cells in which *gur-3* might function, we examined the expression pattern of *gur-3* using a transcriptional reporter (*gur-3_{prom}::gfp*). We observed fluorescence in the I2 and I4 pharyngeal neurons, as well as in the AVD head neurons (Figure 3A). We occasionally observed weaker expression in the PVC tail neurons (data not shown). Functions for the I2 and I4 neurons have not been previously described. To test whether either of the pharyngeal neuron classes might function in the response to light, we used laser microsurgery to kill the pair of I2 neurons and the I4 neuron. We found that killing the I2 neuron pair delayed the acute response, indicating that the I2 neurons promote acute response speed (Figures 3B and 3D). Cell-specific genetic ablation of the I2 neurons using the caspase CSP-1B (Denning et al., 2013) confirmed these findings (Figures S1B and S1D). Furthermore, the analysis of pumping using high-frame-rate videos confirmed that real-time scoring by eye had sufficient accuracy to score the acute response defect in I2-ablated worms (Figures S1C and S1D). By contrast, we observed no effect of ablating the I4 neuron (Figures 3C and 3D).

To determine whether the I2 neurons function in the *lite-1* or *gur-3* pathways, we generated strains in which the I2 neurons were genetically ablated in either the *lite-1* or *gur-3* mutant backgrounds. In the *lite-1* mutant, loss of the I2s resulted in a more defective response to light (Figures 3E and 3G), indicating that *lite-1* and the I2s likely function in parallel pathways. In the *gur-3* mutant, loss of the I2s did not result in a more defective response to light (Figures 3F and 3G), indicating that *gur-3* and the I2s likely function in the same pathway.

To test whether *gur-3* acts in the I2 neurons for the pumping response to light, we generated a transgenic strain (*flp-15_{prom}::mCherry::gur-3*) that expressed a fluorescence-tagged GUR-3 protein using a promoter that expresses specifically in the I2s and PHAs, a pair of neurons in the tail (*flp-15_{prom}* (Kim and Li, 2004)). Expression of *gur-3* using this promoter rescued the acute response defect of *gur-3* mutants (Figures 3H and 3I). These data, together with the expression of *gur-3* in the I2s, indicate that *gur-3* functions cell-autonomously in the I2 neurons for the pumping response to light.

The I2 neurons respond to light in a *gur-3*-dependent manner

To determine if the I2 neurons transduce a light-dependent signal, we generated transgenic *C. elegans* strains that express the genetically-encoded calcium sensor GCaMP3 (Tian et al., 2009) under the *flp-15* promoter. The I2 neurons showed a rapid and robust increase in GCaMP3 fluorescence in response to light (Figure 4A and Movie S2). The GCaMP3 response appeared most quickly and most strikingly in the posterior neurite of I2, beginning within 200 ms and peaking after about 600 ms with a 300% fluorescence increase (Figure 4B). To test whether the spectral sensitivities of the I2 calcium and the pumping responses are similar, we varied the wavelength and power of light used to stimulate the I2 neurons (Figure 4C). To achieve a calcium increase of 50% required 0.8 mW/mm² of 350 nm light, 2.3 mW/mm² of 400 nm light, 3 mW/mm² of 450 nm light, and 7 mW/mm² of 500 nm light. Like the behavioral response, the calcium increase involving the shortest wavelength of light (350 nm) required the lowest power to reach threshold.

Since *gur-3* is required for I2 function in light-induced pumping inhibition, we examined whether *gur-3* is also required for the I2 calcium response. We found that *gur-3* mutants completely lacked the I2 calcium response to light and that this response was restored by I2-specific expression of *gur-3* (Figures 4D, 4E and 4G), indicating that *gur-3* functions in the I2s upstream of its calcium response. By contrast, *lite-1* mutants retained a normal I2 calcium response to light (Figures 4F and 4G). The I2 neurons appeared healthy in *gur-3* mutants: nuclear morphology by Nomarski microscopy looked normal, and baseline GCaMP3 levels were no different than those in the wild type (Figure S7).

Since *gur-3* was required for the I2 calcium response to light, we tested whether other *gur-3*-expressing neurons also responded to light. We generated a strain expressing GCaMP3 under the *gur-3* promoter and observed a calcium increase in the I4 neuron in response to light (Figure S8). AVD did not express GCaMP3 in this strain and was not tested.

GUR-3 confers light-sensitivity to light-insensitive neurons and muscle

We next sought to determine whether GUR-3 could act cell-autonomously to endow light-insensitive cells with light-sensitivity, evidence that would support the hypothesis that GUR-3 functions as a molecular sensor. First, we identified three neuron classes that neither respond to light nor normally express *lite-1* or *gur-3* in wild-type animals, and we expressed *gur-3* in these neurons. Expression of *gur-3* in the AWC and AWB sensory neurons (using the *odr-1/gcy-10* promoter (Yu et al., 1997)) reliably caused increased calcium in response to light (Figures 4H, 4I and 4K). Expression of *gur-3* in the URX sensory neurons (using the *gcy-36* promoter (Yu et al., 1997)) caused 42% (5 of 12) of neurons tested to increase calcium in response to light (Figures 4J and 4K). Second, we used the behavioral output of egg-laying to infer whether the HSN egg-laying neurons were activated by light after HSN-specific *gur-3* expression. Light did not cause wild-type worms to lay eggs, but after *gur-3* was expressed in the HSNs (using the *egl-6a* promoter (Ringstad and Horvitz, 2008)), light reliably evoked egg-laying events (Figure 4L). Third, we tested whether *gur-3* could confer light-sensitivity to a non-neuronal tissue. Body-wall muscle functions in the rapid avoidance of light that wild-type worms exhibit, and we speculated that ectopic expression of a light sensor in body-wall muscle would cause a loss of coordination in this escape response. In fact, *gur-3* expression in body-wall muscle (using the *myo-3* promoter (Okkema et al., 1993)) caused the escape response to be disrupted: worms slowed and sometimes paralyzed in response to light (Figure 4M). Together, these results indicate that GUR-3 can endow a normally light-insensitive cell with light-sensitivity, supporting the hypothesis that GUR-3 functions as a molecular sensor of light or a light-produced product (see below).

Sunlight can inhibit feeding in a *lite-1*-dependent manner

Although it is difficult to compare laboratory conditions with natural conditions, the light used in the experiments described above appears to be substantially brighter (4x-100x) than sunlight (Reference Solar Spectral Irradiance). We found that sunlight was also able to inhibit feeding (Figures S9A and S9E), albeit with a longer latency (30 s) than that caused by the bright light used in the laboratory (1 s). The pumping inhibition caused by sunlight was entirely dependent on *lite-1* (Figures S9B and S9E), as was the locomotory avoidance we also observed in response to sunlight (data not shown). Pumping was still inhibited after loss of *gur-3* or the I2 neurons (Figures S9C-S9E). These results suggest that the *lite-1* pathway can function in the natural light response, but that *gur-3* and the I2 neurons likely function naturally in a different capacity.

Hydrogen peroxide elicits feeding inhibition and locomotory avoidance

Since light can generate hydrogen peroxide (H_2O_2) in solution (Richardson, 1893; Bedford, 1927; Blum, 1932), especially in the presence of biological photosensitizers such as riboflavin, tryptophan and tyrosine (McCormick et al., 1976; Wang and Nixon, 1978), and since LITE-1 and GUR-3 are members of a gustatory receptor family, we hypothesized that *C. elegans* might be responding to the hydrogen peroxide generated by bright light. Using a hydrogen peroxide-sensitive electrode, we observed that light could generate hydrogen peroxide in solution that included riboflavin (Figure 5A). The signal observed by the electrode was confirmed to be hydrogen peroxide because in the presence of catalase it was

severely attenuated (Figure 5B). We did not observe a light-induced signal from the electrode in the absence of riboflavin (data not shown).

Since light-induced hydrogen peroxide can be dependent on riboflavin, we sought to reduce levels of riboflavin in the worm and see if there was any effect on the behavioral response to light. Like humans, *C. elegans* relies on ingestion of riboflavin from its food source to meet endogenous requirements. The *C. elegans* genome encodes two riboflavin transporters homologous to human RFT2, *rft-1* and *rft-2* (Biswas et al., 2013). Because null mutants of *rft-1* and *rft-2* are unavailable, likely because of sterility or lethality, we attempted to reduce levels of expression using RNA interference (RNAi) (Timmons and Fire, 1998). RNAi against either *rft-1* or *rft-2* produced a defect in the feeding response to light (Figures 5C-5E). Since riboflavin is biochemically upstream of many compounds, it is possible that the defect seen after riboflavin reduction was indirect and a consequence of the combined loss of many compounds acting together. Nonetheless, since riboflavin alone is sufficient to generate hydrogen peroxide in response to light, a simple interpretation is that riboflavin itself is required for at least part of the behavioral response to light. In short, these data are consistent with the hypothesis that worms detect hydrogen peroxide generated by light in the light-mediated inhibition of pumping, although they do not definitively prove this hypothesis.

We next sought to determine whether hydrogen peroxide itself can affect worm behavior. When we provided vapor from hydrogen peroxide liquid, worms exhibited a behavioral response strikingly similar to that elicited by light: they stopped pumping and avoided the space containing hydrogen peroxide (Figures 5F-5H). Dosage analysis of the response to liquid hydrogen peroxide revealed that hydrogen peroxide inhibited pumping at concentrations as low as 10 μ M and caused avoidance at concentrations as low as 10 mM. 100 μ M to 1 mM hydrogen peroxide is toxic to *C. elegans* (Jansen et al., 2002).

We imaged calcium in the I2 neurons using GCaMP3 to determine if these neurons responded to hydrogen peroxide vapor as they did to light. The I2 neurons indeed showed an increase in calcium in response to hydrogen peroxide (Figure 5I). Prior to exposure to hydrogen peroxide, the posterior neurite displayed a significant increase in fluorescence in response to the low-power light used for imaging; such a response was not observed in the soma or anterior neurite. After the subtraction of pre-hydrogen peroxide activity from activity during hydrogen peroxide exposure, the responses in all three compartments were equivalent (data not shown).

We next sought to determine if other taste stimuli might activate the I2 neurons. We imaged I2 calcium in response to liquid drops of tastants applied to the worm's head. Unlike the response seen to hydrogen peroxide, exposure of the worm to compounds that were sweet (trehalose, sucrose), bitter (caffeine, quinine), acidic (acetic acid), salty (sodium chloride), and metallic (copper chloride) did not result in activation of the I2 neurons (Figure 5J).

Since both light and hydrogen peroxide activate the I2 neurons, it was conceivable that other environmental insults might also activate the I2 neurons via the generation of hydrogen peroxide. To test this possibility, we imaged the I2 neurons after exposure to additional

insults. We exposed the worm to osmotic shock (2 M glycerol), detergent stress (0.1% SDS), protein synthesis block (cyclohexamide), and oxidizers (potassium dichromate and potassium permanganate) and found that these stimuli did not activate I2 (Figure 5J). Exposure to the superoxide-generator paraquat (1 M) and the oxidizer sodium hypochlorite (750 mM) did activate I2, albeit at concentrations ~100x higher than the 10 mM hydrogen peroxide sufficient to drive a response in this assay. Although it is difficult to interpret the results of exposure to such high concentrations of any compound, we suggest that the I2 neurons are specifically sensitive to stimuli that can cause oxidation, particularly hydrogen peroxide. The I2 neurons do not seem to be sensitive to tastants or toxins more generally.

Avoidance of hydrogen peroxide requires *lite-1*, and feeding inhibition requires *gur-3* and *lite-1*

We sought to determine whether *lite-1* or the I2 pathway, including *gur-3*, was responsible for the inhibition of pumping in response to hydrogen peroxide. As with light, *lite-1* mutants failed to avoid hydrogen peroxide at all concentrations tested (Figure 6G). However, they continued to inhibit pumping in response to hydrogen peroxide (Figures 6A, 6E and 6F). By contrast, *gur-3* mutants exhibited a defective acute response to hydrogen peroxide (Figures 6B, 6E and 6F). Furthermore, the *lite-1 gur-3* double mutant was nearly completely defective in the pumping response to hydrogen peroxide (Figures 6C, 6E and 6F), indicating that *lite-1* also functions in the pumping response to hydrogen peroxide.

Synergistic genetic interactions, like that shown between *lite-1* and *gur-3* in the pumping response to hydrogen peroxide, generally reflect redundant functions. For example, either of two single mutants can be phenotypically wild-type while the double mutant is grossly abnormal if the function of either gene is sufficient for a normal phenotype. In the case of *lite-1* and *gur-3*, we interpret our observations as indicating partially redundant function with the function of *gur-3* being more important than that of *lite-1*. More specifically, we suggest that GUR-3 functions to inhibit feeding at both low and high concentrations of hydrogen peroxide and that LITE-1 functions to inhibit feeding only at high concentrations, at or above 10 mM hydrogen peroxide. Two considerations support this proposal: (1) *gur-3* mutants did not inhibit feeding in response to hydrogen peroxide concentrations less than 10 mM but did inhibit feeding somewhat at higher concentrations, and (2) the *lite-1 gur-3* double mutant was nearly completely defective at all concentrations tested. These findings indicate that the hydrogen peroxide-induced feeding inhibition that occurs in the absence of GUR-3 is mediated by LITE-1. We postulate that the *lite-1* single mutant does not exhibit a defect in pumping inhibition because hydrogen peroxide continues to activate GUR-3, which mediates sensitivity to both low and high concentrations of hydrogen peroxide. *gur-3* mutants exhibited a defect because LITE-1 is unable to compensate, as LITE-1 mediates sensitivity to only high concentrations of hydrogen peroxide. Worms lacking the I2 neurons also exhibited a defect in the acute pumping response to hydrogen peroxide similar to the defect observed in response to light (Figures 6D-F).

As with the response to light, *gur-3* was required for the I2 calcium increase in response to hydrogen peroxide (Figures 6H and 6I), as well as for the response to paraquat and bleach (Figure S10). Taken together, these results indicate that the gustatory receptor orthologs

lite-1 and *gur-3* and the I2 pharyngeal neurons function in the inhibition of feeding in response to hydrogen peroxide.

The peroxiredoxin PRDX-2 functions in I2 in the response to light and hydrogen peroxide

To identify additional molecular components in the sensing of hydrogen peroxide, we tested antioxidant genes that might function in this response. Catalases and peroxiredoxins are evolutionarily conserved antioxidant enzymes known to directly reduce hydrogen peroxide. The *C. elegans* genome encodes three catalases (*ctl-1*, *ctl-2* and *ctl-3*) and three peroxiredoxins (*prdx-2*, *prdx-3* and *prdx-6*). While loss of catalase by mutation of *ctl-1(ok1242)*, *ctl-2(ok1137)* or *ctl-3(ok2042)* or loss of peroxiredoxin by mutation of *prdx-3(gk529)* and *prdx-6(tm4225)* did not affect the acute response to light (Figures S11A-S11E), the *prdx-2(gk169)* mutant had a defect in the acute pumping response similar to that caused by *gur-3* mutation and I2 ablation (Figures 7A and 7F). *C. elegans* PRDX-2 is 72% identical to human PRDX1 and PRDX2.1. Like the *lite-1 gur-3* double mutant, the *prdx-2; lite-1* double mutant was severely defective in the feeding response to light, substantially more defective than either single mutant (Figures 7B and 7F). The *prdx-2; gur-3* double mutant did not enhance the acute response defect of the *gur-3* single mutant (Figure S11F), suggesting that *prdx-2* and *gur-3* likely function in the same pathway.

Examination of the expression pattern of *prdx-2* using a rescuing translational reporter (*prdx-2_{prom}::prdx-2::mCherry*) revealed expression in a broad set of tissues: I2, I4 and intestine (as previously reported (Isermann et al., 2004)), as well as muscle (pharyngeal muscle 1, vulval muscle, body wall muscle), epithelial cells (e1, e3), and many neurons in the head and tail (Figures 7C and 7D). To test whether *prdx-2* acts in the I2 neurons for the pumping response to light, we generated a transgenic strain that expresses *prdx-2* cDNA specifically in the I2s (*flp-15_{prom}::prdx-2 cDNA*). I2-specific expression of *prdx-2* rescued the acute response defect of *prdx-2* mutants (Figures 7E and 7F), indicating that *prdx-2* functions in I2 for the pumping response to light.

Since *prdx-2* is required for the function of the I2 neurons in light-induced pumping inhibition, we examined whether *prdx-2* is also required for the I2 calcium response. We found that *prdx-2* mutants completely lacked the I2 calcium response to light and that this response was restored by I2-specific expression of *prdx-2* (Figures 7G-7I). The I2 neurons appeared healthy in *prdx-2* mutants: nuclear morphology by Nomarski microscopy looked normal, and baseline GCaMP3 levels were no different than wild-type (Figure S7).

As with light, *prdx-2* mutants were defective in the acute response to hydrogen peroxide vapor (Figures 8A and 8C), and the *prdx-2; lite-1* double mutant was severely defective in the pumping response to hydrogen peroxide (Figures 8B and 8C). *prdx-2* mutants were also defective in the pumping response to liquid hydrogen peroxide (Figure 8D). *prdx-2* mutants also showed a defective I2 response to hydrogen peroxide vapor (Figures 8E and 8F). Taken together, these results show that the conserved peroxiredoxin *prdx-2* functions in I2 to facilitate the I2 neuron's response to both light and hydrogen peroxide.

DISCUSSION

By analyzing the effect of light on the feeding behavior of *C. elegans*, we have discovered a gustatory pathway for responding to the reactive oxygen species hydrogen peroxide. We showed that worms inhibit feeding and promote locomotory avoidance in response to hydrogen peroxide and that these behaviors rely on two members of the gustatory receptor family in *C. elegans*, GUR-3 and LITE-1. The I2 pharyngeal neurons are activated by hydrogen peroxide and inhibit feeding in response to hydrogen peroxide. I2 activation by hydrogen peroxide requires GUR-3 as well as PRDX-2, an antioxidant enzyme peroxiredoxin.

We speculate that GUR-3, as a member of the gustatory receptor family, functions as a receptor for hydrogen peroxide (or a product of a chemical reaction involving hydrogen peroxide), since members of this family in insects have been shown to function as direct receptors for their tastants: GR5A senses trehalose (Chyb et al., 2003), and BmGR-9 and GR43A sense fructose (Sato et al., 2011). Similarly, we speculate that LITE-1, also a member of the gustatory receptor family, functions as a receptor for a reactive oxygen species (or a product of a chemical reaction involving a reactive oxygen species). We propose that the LITE-1 ligand is not hydrogen peroxide, because LITE-1 is required for behavioral responses to hydrogen peroxide of relatively high concentrations (greater than or equal to 10 mM) while GUR-3 is required for the pumping response to hydrogen peroxide of lower concentrations (greater than or equal to 10 μ M). Locomotory avoidance of hydrogen peroxide is activated by concentrations greater than or equal to 10 mM and requires LITE-1, and pumping inhibition activated by greater than or equal to 10 mM hydrogen peroxide also requires LITE-1. Thus, LITE-1 appears to function in a low-affinity pathway responsible for detecting millimolar hydrogen peroxide while GUR-3 functions in a high-affinity pathway for detecting micromolar hydrogen peroxide. Although others have speculated that LITE-1 functions as a photoreceptor on the basis of experiments involving ectopic expression in *C. elegans* (Edwards et al., 2008; Liu et al., 2010), we suspect that the mechanism by which LITE-1 detects light involves the generation of an oxidant other than hydrogen peroxide. Similar speculation applies to GR28B, an ortholog of LITE-1 that was implicated in photoreception by *Drosophila* larvae (Xiang et al., 2010). Recently, UVC light (254 nm, 0.012 mW/mm²) was shown to cause a writhing response in *Drosophila* larvae, likely via the generation of reactive oxygen species (Kim and Johnson, 2014). Future work is needed to establish the mechanism by which GUR-3 and LITE-1 function in the detection of reactive oxygen species.

Since LITE-1 is required for responses to sunlight, we believe that the generation of reactive oxygen species by light is likely the mechanism by which LITE-1 detects environmental light. The GUR-3 pathway, on the other hand, is activated only by unnaturally bright light, and we suggest that this pathway naturally functions in the environmental detection of hydrogen peroxide and/or other reactive oxygen species and not in the detection of natural light.

We have also identified a role for the peroxiredoxin PRDX-2 in hydrogen peroxide-sensing. Peroxiredoxins are a family of enzymes directly oxidized by hydrogen peroxide and have

been shown to have both peroxidase and signaling functions (Rhee et al., 2012; Marinho et al., 2014). As a peroxidase, peroxiredoxin can protect cells from oxidative stress by degrading hydrogen peroxide. If PRDX-2 were playing such a role in the inhibition of feeding by hydrogen peroxide, loss of *prdx-2* would be expected to increase hydrogen peroxide levels and therefore enhance the response to hydrogen peroxide. However, we observed the opposite effect: loss of *prdx-2* led to a decrease in response, suggesting that PRDX-2 does not simply function as a peroxidase in the inhibition of feeding by hydrogen peroxide. As a signaling molecule, peroxiredoxin can function either directly with hydrogen peroxide as a peroxidase oxidizer or indirectly as a reducing agent. For example, as a peroxidase signaler, peroxiredoxin can be the initial sensor of hydrogen peroxide and transfer its thiol-disulfide to oxidize and activate a target protein, as shown for the Yap1 transcription factor (Tachibana et al., 2009) and the ASK1 kinase (Jarvis et al., 2012). As a reducing agent signaler, peroxiredoxin might reduce an oxidized compound produced in the sensory pathway for hydrogen peroxide, such as an oxidized ligand or receptor. Such a role is supported by evidence that the bacterial peroxiredoxin AhpC can function as a disulfide reductase (Ritz et al., 2001) and that human Prdx1 activates the neuronal transmembrane protein GDE2 by disulfide reduction (Yan et al., 2009). Because GUR-3 is a neuronal transmembrane protein, we favor a model in which peroxiredoxin functions in signal transduction by disulfide reduction. We propose that PRDX-2 functions in acute detection of hydrogen peroxide by reducing a molecule, such as GUR-3, that is oxidized in the process of sensory transduction. Further studies are needed to explore these two signaling models for PRDX-2 function.

Interestingly, peroxiredoxins are present in the retina (Klebe et al., 2014; Moreira et al., 2008), and the light intensity at the level of the retina (after focusing by the cornea and lens) is within the range studied here (Liang et al., 1997). We speculate that the light-generation of reactive oxygen species we propose mediates the response of *C. elegans* to light might also occur in the retina. It would be interesting to determine the role, if any, that peroxiredoxins might play in retinal light transduction.

Although known for some time, the generation of reactive oxygen species by light is worth highlighting, given the widespread use of optogenetics for the observation and manipulation of neural activity (Tian et al., 2009; Boyden et al., 2005). The light intensities typically used for channelrhodopsin activation of neurons in mice is 10-20 mW/mm² of 473 or 488 nm light (Arenkiel et al., 2007; Gunaydin et al., 2014). These wavelengths and intensities of light activate the *C. elegans* I2 neurons we have studied and would be expected to generate hydrogen peroxide in mouse brain if the concentration of photosensitizers, such as riboflavin, is similar to that in *C. elegans*. In other words, the light used in optogenetic experiments might cause oxidative stress and consequently interfere with endogenous neural activity. There is evidence that reactive oxygen species can affect neural functions, such as long-term potentiation (Kamsler and Segal, 2003). We suggest that researchers be cognizant of the fact that optogenetic light might generate reactive oxygen species *in vivo*, and for that reason might confound the interpretation of data obtained using the optogenetic method.

Although *C. elegans* has not been reported to encounter hydrogen peroxide in the wild, it is possible that these nematodes could encounter both environmental and biological sources of

hydrogen peroxide. Rain water can contain hydrogen peroxide as high as 200 μM (ECETOC, 1996). Additionally, the pathogenic bacteria *Streptococcus* and *Enterococcus* can kill *C. elegans* by producing lethal levels of hydrogen peroxide as high as 2 mM (Jansen et al., 2002; Bolm et al., 2004; Moy et al., 2004). Other bacteria, such as *Lactobacillus*, also produce hydrogen peroxide (Collins and Aramaki, 1980). In addition, hydrogen peroxide is found in human tissue, with concentrations as high as 600 μM in the aqueous humour of the eye (ECETOC, 1996). Finally, bombardier beetles can produce hydrogen peroxide of very high concentration, up to 8 M (ECETOC, 1996). Our results show that feeding is inhibited by as little as 10 μM hydrogen peroxide, which indicates that *C. elegans* would be responsive to such environmental and biological sources of hydrogen peroxide. If *C. elegans* ingests pathogenic bacteria, one survival strategy might be to detect hydrogen peroxide at the level of the pharynx and inhibit feeding using the mechanism we describe above.

By identifying a gustatory pathway for a stimulus other than the five main tastes, our results support the notion that additional taste pathways exist. Others have speculated about the existence of taste pathways for astringents and metals (Chaudhari and Roper, 2010). We suggest that studying the detection of non-canonical gustatory stimuli will expand our understanding of the ways in which animals sense and respond to their environments.

EXPERIMENTAL PROCEDURES

Complete Experimental Procedures are available in Supplemental Information.

Behavioral responses to light and hydrogen peroxide

1-day post-L4 adult worms were assayed. For responses to artificial light, pumping was scored by eye using a stereo dissecting microscope at magnification of 120x and illuminated with a halogen light. Light stimulation was at 436 nm and 13 mW/mm² and supplied via a cyan fluorescent protein (CFP) filter, unless stated otherwise. Custom Matlab software (available at <http://www.wormweb.org>) recorded the timing of pumps as indicated by manual key presses and controlled a shutter that presented and removed arc-lamp illumination. For responses to sunlight, worms were taken outside and maintained in the shade. During sunlight exposure, worms were exposed to direct sunlight. To assess the spectral response, worms were picked to an NGM agar pad on a cover slip and viewed using an inverted microscope with a 20x objective. The wavelength was controlled via a diffraction grating. For behavioral responses to heat, a hot-air gun was used to heat the surface of a plate with worms on it. For responses to hydrogen peroxide, the worms were exposed to either vapor from 30% hydrogen peroxide (8.82 M) loaded in a needle or drops of hydrogen peroxide released from a needle or pipette.

Laser ablations

A pulsed nitrogen laser was used to ablate individual pharyngeal neurons identified by Nomarski differential interference contrast optics. Worms were at the L1 or L2 stage, and ablations were confirmed the following day. On day three, adult worms were assayed behaviorally.

Calcium imaging

Calcium was assessed using a GCaMP genetically-encoded calcium indicator, either GCaMP or GCaMP3 (Tian et al., 2009). GCaMP3 was expressed in the I2 neurons using the *flp-15* promoter. Adult worms were immobilized using polystyrene beads on 10% agarose pads under a cover slip (Kim et al., 2013), and neurons were imaged and stimulated simultaneously using 26 mW/mm² 485 nm light using an inverted microscope with a 40x air objective. Videos were recorded using an EMCCD camera and analyzed using custom Matlab software (available at <http://www.wormweb.org>). To expose the I2 neurons to vapor or liquid stimuli, worms were glued to NGM agar pads using cyanoacrylate glue. Imaging was conducted at lower power (2 mW/mm²) and reduced exposure time (100-200 ms, 1fps) to minimize activation of the I2 neuron by the imaging light. GCaMP3 or GCaMP was also used to assess the response to light in the AWC, AWB and URX neurons with or without ectopic *gur-3* expression.

Expression analysis

Gene expression was examined using transgenes fused to a fluorescent protein (GFP or mCherry). A confocal microscope was used to generate image stacks, from which a maximum-intensity projection was used to generate the images shown.

Supplementary Material

Refer to Web version on PubMed Central for supplementary material.

ACKNOWLEDGEMENTS

We thank N. An, T. Hirose, D. Denning, K. Miller, S. Xu, Z. Hu, J. Kaplan, C. Bargmann, S. Mitani, the *Caenorhabditis* Genetics Center and Addgene for strains and reagents; N. Ringstad, S. Nakano, D. Ma, N. Paquin, C. Engert, S. Luo, D. Pagano, S. Sando and K. Boulias for discussions and advice; and D. Ma, D. Denning, N. Paquin, K. Birkhart, V. O'Connor, N. Dalliere, D. Pagano, S. Sando and K. Boulias for review of the manuscript. N.B. was supported by a National Science Foundation Graduate Research Fellowship. This work was supported by NIH grant GM24663 to H.R.H. H.R.H. is an Investigator of the Howard Hughes Medical Institute.

REFERENCES

- Arenkiel B, Peca J, Davison I, Feliciano C, Deisseroth K, Augustine G, Ehlers M, Feng G. In vivo light-induced activation of neural circuitry in transgenic mice expressing channelrhodopsin-2. *Neuron*. 2007; 54:205–218. [PubMed: 17442243]
- Bedford T. The nature of the action of ultra-violet light on micro-organisms. *British Journal of Experimental Pathology*. 1927; 8:437–444.
- Biswas A, Elmatari D, Rothman J, LaMunyon C, Said H. Identification and functional characterization of the *Caenorhabditis elegans* riboflavin transporters *rft-1* and *rft-2*. *PLoS One*. 2013; 8:e58190. [PubMed: 23483992]
- Blum H. Photodynamic action. *Physiological Review*. 1932:23–55.
- Bolm M, Jansen W, Schnabel R, Chhatwal G. Hydrogen peroxide-mediated killing of *Caenorhabditis elegans*: a common feature of different Streptococcal species. *Infection and Immunity*. 2004; 72:1192–1194. [PubMed: 14742574]
- Boyden E, Zhang F, Bamberg E, Nagel G, Deisseroth K. Millisecond-timescale, genetically targeted optical control of neural activity. *Nature Neuroscience*. 2005; 8:1263–1268.
- Cameron P, Hiroi M, Ngai J, Scott K. The molecular basis for water taste in *Drosophila*. *Nature*. 2010; 465:91–95. [PubMed: 20364123]

- Cartoni C, Yasumatsu K, Ohkuri T, Shigemura N, Yoshida R, Godinot N, le Coutre J, Ninomiya Y, Damak S. Taste preference for fatty acids is mediated by GPR40 and GPR120. *The Journal of Neuroscience*. 2010; 30:8376–8382. [PubMed: 20573884]
- Chandrashekar J, Yarmolinsky D, von Buchholtz L, Oka Y, Sly W, Ryba N, Zuker C. The taste of carbonation. *Science*. 2009; 326:443–445. [PubMed: 19833970]
- Chaudhari N, Roper S. The cell biology of taste. *The Journal of Cell Biology*. 2010; 190:285–296. [PubMed: 20696704]
- Chen Z, Wang Q, Wang Z. The amiloride-sensitive epithelial sodium channel PPK28 is essential for *Drosophila* gustatory water reception. *The Journal of Neuroscience*. 2010; 30:6247–6252. [PubMed: 20445050]
- Chyb S, Dahanukar A, Wickens A, Carlson J. *Drosophila Gr5a* encodes a taste receptor tuned to trehalose. *Proceedings of the National Academy of Sciences*. 2003; 100:14526–14530.
- Cina S, Downs J, Conradi S. Hydrogen peroxide: A source of lethal oxygen embolism: Case report and review of the literature. *The American Journal of Forensic Medicine and Pathology*. 1994; 15:44–50. [PubMed: 8166115]
- Collins E, Aramaki K. Production of hydrogen peroxide by *Lactobacillus acidophilus*. *Journal of Dairy Science*. 1980; 63:353–357. [PubMed: 6768778]
- Delaunay A, Pglieger D, Barrault M, Vinh J, Toledano M. A thiol peroxidase is an H₂O₂ receptor and redox-transducer in gene activation. *Cell*. 2002; 111:471–481. [PubMed: 12437921]
- Denning D, Hatch V, Horvitz H. Both the caspase CSP-1 and a caspase-independent pathway promote programmed cell death in parallel to the canonical pathway for apoptosis in *Caenorhabditis elegans*. *PLoS Genetics*. 2013; 9:e1003341. [PubMed: 23505386]
- ECETOC. Special Report No. 10 - Hydrogen Peroxide OEL Criteria Document. ECETOC; Brussels, Belgium: 1996.
- Edwards S, Charlie N, Milfort M, Brown B, Gravlin C, Knecht J, Miller K. A novel molecular solution for ultraviolet light detection in *Caenorhabditis elegans*. *PLoS Biology*. 2008; 6:e198. [PubMed: 18687026]
- Fischler W, Kong P, Marella S, Scott K. The detection of carbonation by the *Drosophila* gustatory system. *Nature*. 2007; 448:1054–1057. [PubMed: 17728758]
- Gunaydin L, Grosenick L, Finkelstein J, Kauvar I, Fenno L, Adhikari A, Lammel S, Mirzabekov J, Airan R, Zalocusky K, et al. Natural neural projection dynamics underlying social behavior. *Cell*. 2014; 157:1535–1551. [PubMed: 24949967]
- Horvitz H, Chalfie M, Trent C, Evans P. Serotonin and octopamine in the nematode *Caenorhabditis elegans*. *Science*. 1982; 216:1012–1014. [PubMed: 6805073]
- Isermann K, Liebau E, Roeder T, Bruchhaus I. A peroxiredoxin specifically expressed in two types of pharyngeal neurons is required for normal growth and egg production in *Caenorhabditis elegans*. *Journal of Molecular Biology*. 2004; 338:745–755. [PubMed: 15099742]
- Jansen W, Bolm M, Balling R, Chhatwal G, Schnabel R. Hydrogen peroxide-mediated killing of *Caenorhabditis elegans* by *Streptococcus pyogenes*. *Infection and Immunity*. 2002; 70:5202–5207. [PubMed: 12183571]
- Jarvis R, Hughes S, Ledgerwood E. Peroxiredoxin 1 functions as a signal peroxidase to receive, transduce, and transmit peroxide signals in mammalian cells. *Free Radical Biology and Medicine*. 2012; 53:1522–1530. [PubMed: 22902630]
- Kamsler A, Segal M. Hydrogen peroxide modulation of synaptic plasticity. *The Journal of Neuroscience*. 2003; 23:269–276. [PubMed: 12514224]
- Kim K, Li C. Expression and regulation of an FMRFamide-related neuropeptide gene family in *Caenorhabditis elegans*. *The Journal of Comparative Neurology*. 2004; 475:540–550. [PubMed: 15236235]
- Kim E, Sun L, Gabel C, Fang-Yen C. Long-term imaging of *Caenorhabditis elegans* using nanoparticle-mediated immobilization. *PLoS One*. 2013; 8:e53419. [PubMed: 23301069]
- Kim M, Johnson W. ROS-mediated activation of *Drosophila* larval nociceptor neurons by UVC irradiation. *BMC Neuroscience*. 2014; 15:14. [PubMed: 24433322]

- Klebe S, Callahan T, Power J. Peroxiredoxin I and II in human eyes: Cellular distribution and association with pterygium and DNA damage. *Journal of Histochemistry and Cytochemistry*. 2014; 62:85–96. [PubMed: 24152995]
- Li Z, Li Y, Yi Y, Huang W, Yang S, Niu W, Zhang L, Xu Z, Qu A, Wu Z, et al. Dissecting a central flip-flop circuit that integrates contradictory sensory cues in *C. elegans* feeding regulation. *Nature Communications*. 2012; 3:776.
- Liang J, Williams D, Miller D. Supernormal vision and high-resolution retinal imaging through adaptive optics. *Journal of the Optical Society of America*. 1997; 14:2884–2892. [PubMed: 9379246]
- Liman E, Zhang Y, Montell C. Peripheral coding of taste. *Neuron*. 2014; 81:984–1000. [PubMed: 24607224]
- Lindemann B. Receptors and transduction in taste. *Nature*. 2001; 413:219–225. [PubMed: 11557991]
- Liu J, Ward A, Gao J, Dong Y, Nishio N, Inada H, Kang L, Yu Y, Ma D, Xu T, et al. *C. elegans* phototransduction requires a G protein-dependent cGMP pathway and a taste receptor homolog. *Nature Neuroscience*. 2010; 13:715–722.
- Marinho H, Real C, Cyrne L, Soares H, Antunes F. Hydrogen peroxide sensing, signaling and regulation of transcription factors. *Redox Biology*. 2014; 2:535–562. [PubMed: 24634836]
- Masek P, Keene A. *Drosophila* fatty acid taste signals through the PLC pathway in sugar-sensing neurons. *PLoS Genetics*. 2013; 9:e1003710. [PubMed: 24068941]
- McCormick J, Fischer J, Pachlatko J, Eisenstark A. Characterization of a cell-lethal product from photooxidation of tryptophan: hydrogen peroxide. *Science*. 1976; 191:468–469. [PubMed: 1108203]
- Moreira E, Kantorow M, Rodriguez I. Peroxiredoxin 3 (PRDX3) is highly expressed in the primate retina especially in blue cones. *Experimental Eye Research*. 2008; 86:452–455. [PubMed: 18078932]
- Moy T, Mylonakis E, Calderwood S, Ausubel F. Cytotoxicity of hydrogen peroxide produced by *Enterococcus faecium*. *Infection and Immunity*. 2004; 72:4512–4520. [PubMed: 15271910]
- Okkema P, Harrison S, Plunger V, Aryana A, Fire A. Sequence requirements for myosin gene expression and regulation in *Caenorhabditis elegans*. *Genetics*. 1993; 135:385–404. [PubMed: 8244003]
- Reference Solar Spectral Irradiance: ASTM G-173 (<http://rredc.nrel.gov/solar/spectra/am1.5/ASTMG173/ASTMG173.html>)
- Rhee S, Woo H, Kil I, Bae S. Peroxiredoxin functions as a peroxidase and a regulator and sensor of local peroxides. *The Journal of Biological Chemistry*. 2012; 287:4403–4410. [PubMed: 22147704]
- Richardson A. The action of light in preventing putrefactive decomposition; and in inducing the formation of hydrogen peroxide in organic liquids. *Journal of the Chemical Society, Transactions*. 1893; 63:1109–1130.
- Ringstad N, Horvitz H. FMRFamide neuropeptides and acetylcholine synergistically inhibit egg-laying by *C. elegans*. *Nature Neuroscience*. 2008; 11:1168–1176.
- Ritz D, Lim J, Reynolds C, Poole L, Beckwith J. Conversion of a peroxiredoxin into a disulfide reductase by a triplet repeat expansion. *Science*. 2001; 294:158–160. [PubMed: 11588261]
- Robertson H, Warr C, Carlson J. Molecular evolution of the insect chemoreceptor gene superfamily in *Drosophila melanogaster*. *Proceedings of the National Academy of Sciences*. 2003; 100:14537–14542.
- Sandell M, Breslin P. Variability in a taste-receptor gene determines whether we taste toxins in food. *Current Biology*. 2006; 16:R792–R794. [PubMed: 16979544]
- Sato K, Tanaka K, Touhara K. Sugar-regulated cation channel formed by an insect gustatory receptor. *Proceedings of the National Academy of Sciences*. 2011; 108:11680–11685.
- Storz G, Tartaglia L, Ames B. Transcriptional regulator of oxidative stress-inducible genes: Direct activation by oxidation. *Science*. 1990; 248:189–194. [PubMed: 2183352]
- Tachibana T, Okazaki S, Murayama A, Naganuma A, Nomoto A, Kuge S. A major peroxiredoxin-induced activation of Yap1 transcription factor is mediated by reduction-sensitive disulfide bonds and reveals a low level of transcriptional activation. *The Journal of Biological Chemistry*. 2009; 284:4464–4472. [PubMed: 19106090]

- Tian L, Hires S, Mao T, Huber D, Chiappe M, Chalasani S, Petreanu L, Akerboom J, McKinney S, Schreiter E, et al. Imaging neural activity in worms, flies and mice with improved GCaMP calcium indicators. *Nature Methods*. 2009; 6:875–881. [PubMed: 19898485]
- Timmons L, Fire A. Specific interference by ingested dsRNA. *Nature*. 1998; 395:854. [PubMed: 9804418]
- Veal E, Day A, Morgan B. Hydrogen peroxide sensing and signaling. *Molecular Cell*. 2007; 26:1–14. [PubMed: 17434122]
- Wang R, Nixon B. Identification of hydrogen peroxide as a photoproduct toxic to human cells in tissue-culture medium irradiated with “daylight” fluorescent light. *In Vitro*. 1978; 14:715–722. [PubMed: 689707]
- Ward A, Liu J, Feng Z, Xu X. Light-sensitive neurons and channels mediate phototaxis in *C. elegans*. *Nature Neuroscience*. 2008; 11:916–922.
- Wisotsky Z, Medina A, Freeman E, Dahanukar A. Evolutionary differences in food preference rely on Gr64e, a receptor for glycerol. *Nature Neuroscience*. 2011; 14:1534–1541.
- Xiang Y, Yuan Q, Vogt N, Looger L, Jan L, Jan Y. Light-avoidance-mediating photoreceptors tile the *Drosophila* larval body wall. *Nature*. 2010; 468:921–926. [PubMed: 21068723]
- Yan Y, Sabharwal P, Rao M, Sockanathan S. The antioxidant enzyme Prdx1 controls neuronal differentiation by thiol-redox-dependent activation of GDE2. *Cell*. 2009; 138:1209–1221. [PubMed: 19766572]
- Yu S, Avery L, Baude E, Garbers D. Guanylyl cyclase expression in specific sensory neurons: A new family of chemosensory receptors. *Proceedings of the National Academy of Sciences*. 1997; 94:3384–3387.

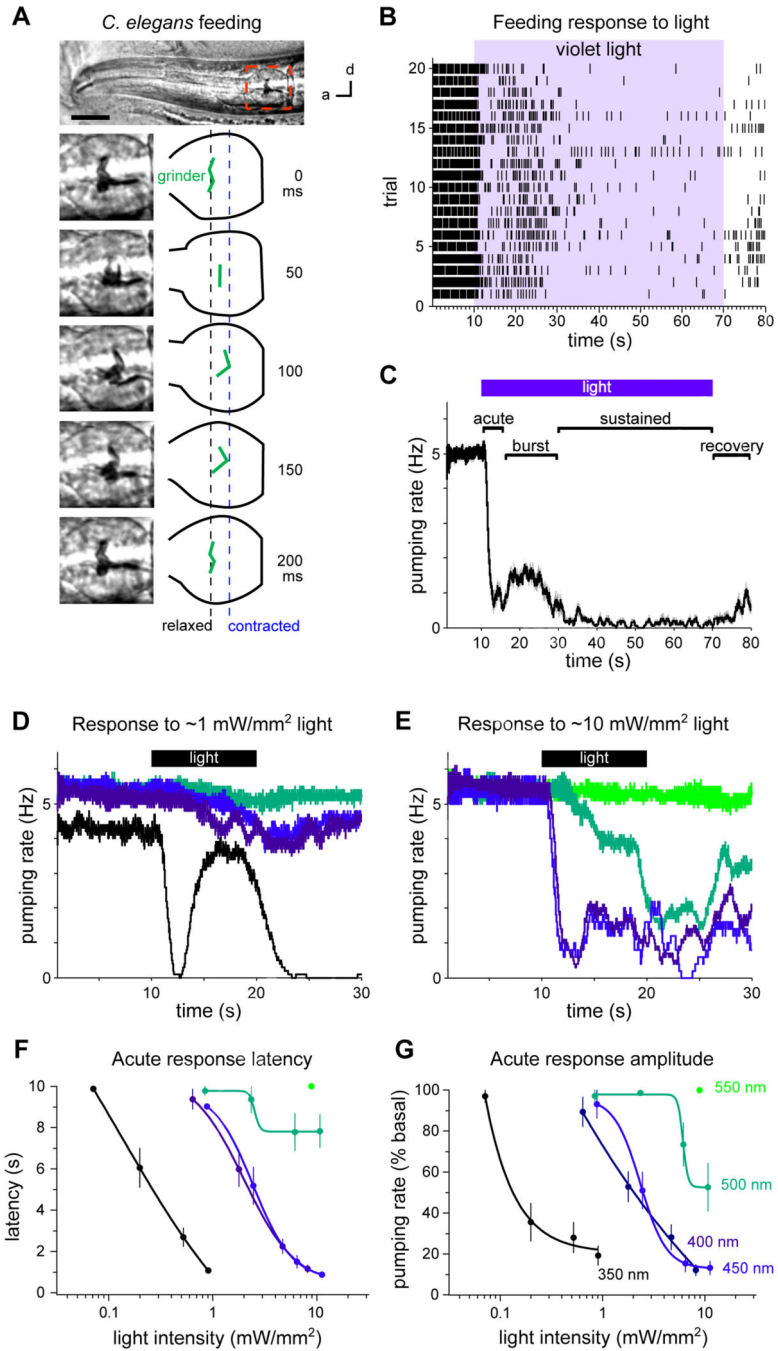


Figure 1. Light inhibits *C. elegans* feeding

(A) Adult *C. elegans* head showing one pump of the grinder. d = dorsal, a = anterior. Scale bar = 20 μ m.

(B) Raster plot of pumps (each tick represents a pump), one trial per row, before, during and after light exposure (436 nm, 13 mW/mm²).

(C) Backward moving average of (B), with the acute, burst, sustained and recovery responses labeled.

(D) Pumping responses to 350 (UVA), 400 (violet), 450 (blue) and 500 nm (green) light of 0.6-0.9 mW/mm². 350 nm light effectively induces the burst response.

(E) Pumping responses to 400, 450, 500 and 550 nm (green) light of 8-11 mW/mm².

(F) Spectral sensitivity of the acute response latency, defined as the time from light onset to first missed pump (see Experimental Procedures).

(G) Spectral sensitivity of the acute response amplitude, defined as the pumping rate after the first missed pump normalized to the pre-light pumping rate (see Experimental Procedures). (D-G) Shorter wavelength light is more potent than longer wavelength light for eliciting the pumping response to light. Colors of lines in (D-G) indicate wavelengths of light, as labeled in (G).

n = 10-20 worms. Shading around traces and error bars indicate s.e.m.

See also Figures S1-S3 and Movie S1.

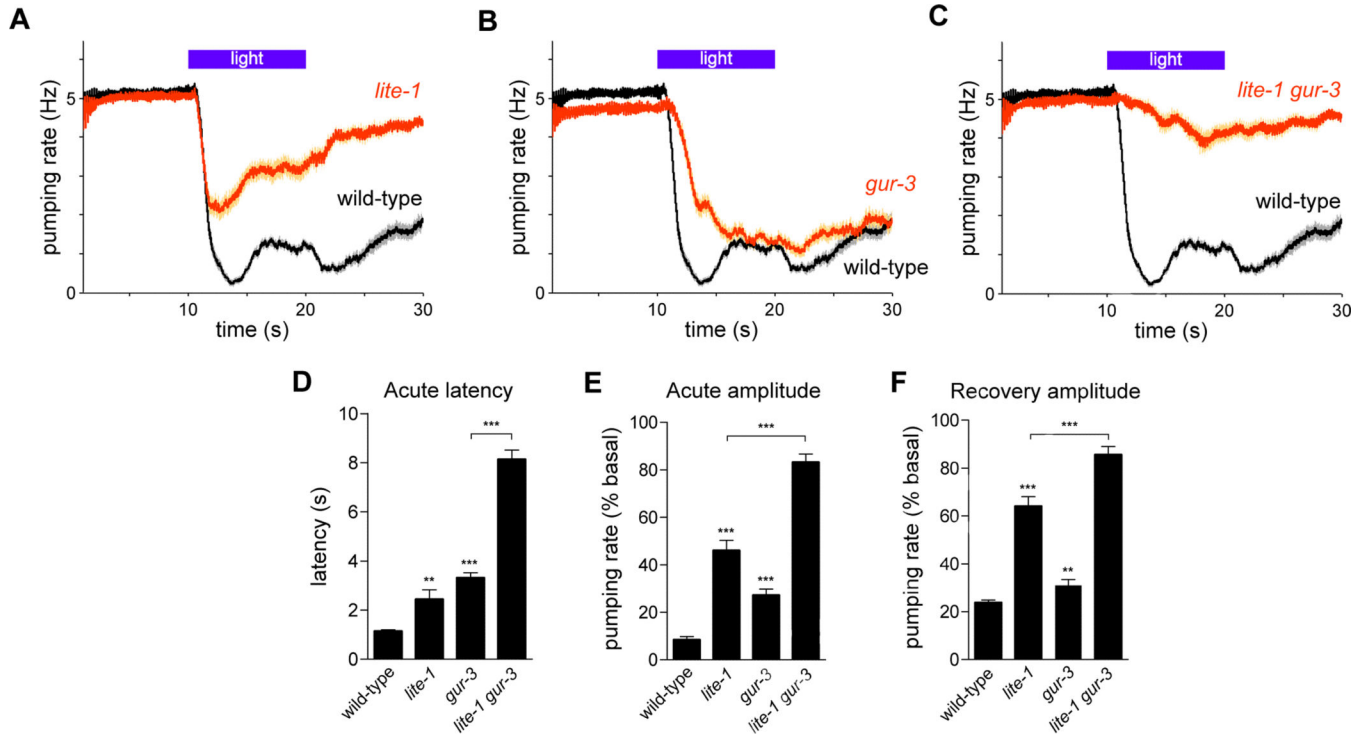


Figure 2. The gustatory receptor orthologs *lite-1* and *gur-3* are required for the feeding response to light

(A) *lite-1*(*ce314*) mutants were defective in the acute and recovery responses to light.

(B) *gur-3*(*ok2245*) mutants were defective in the acute response to light.

(C) *lite-1 gur-3* double mutants were severely defective in the acute and recovery responses to light.

(D) Quantification of acute response latency.

(E) Quantification of acute response amplitude.

(F) Quantification of the recovery response amplitude. n = 60 worms. Shading around traces and error bars indicate s.e.m. ** p < 0.01, *** p < 0.001, t-test, compared to wild-type or indicated strain.

See also Figures S4 and S5.

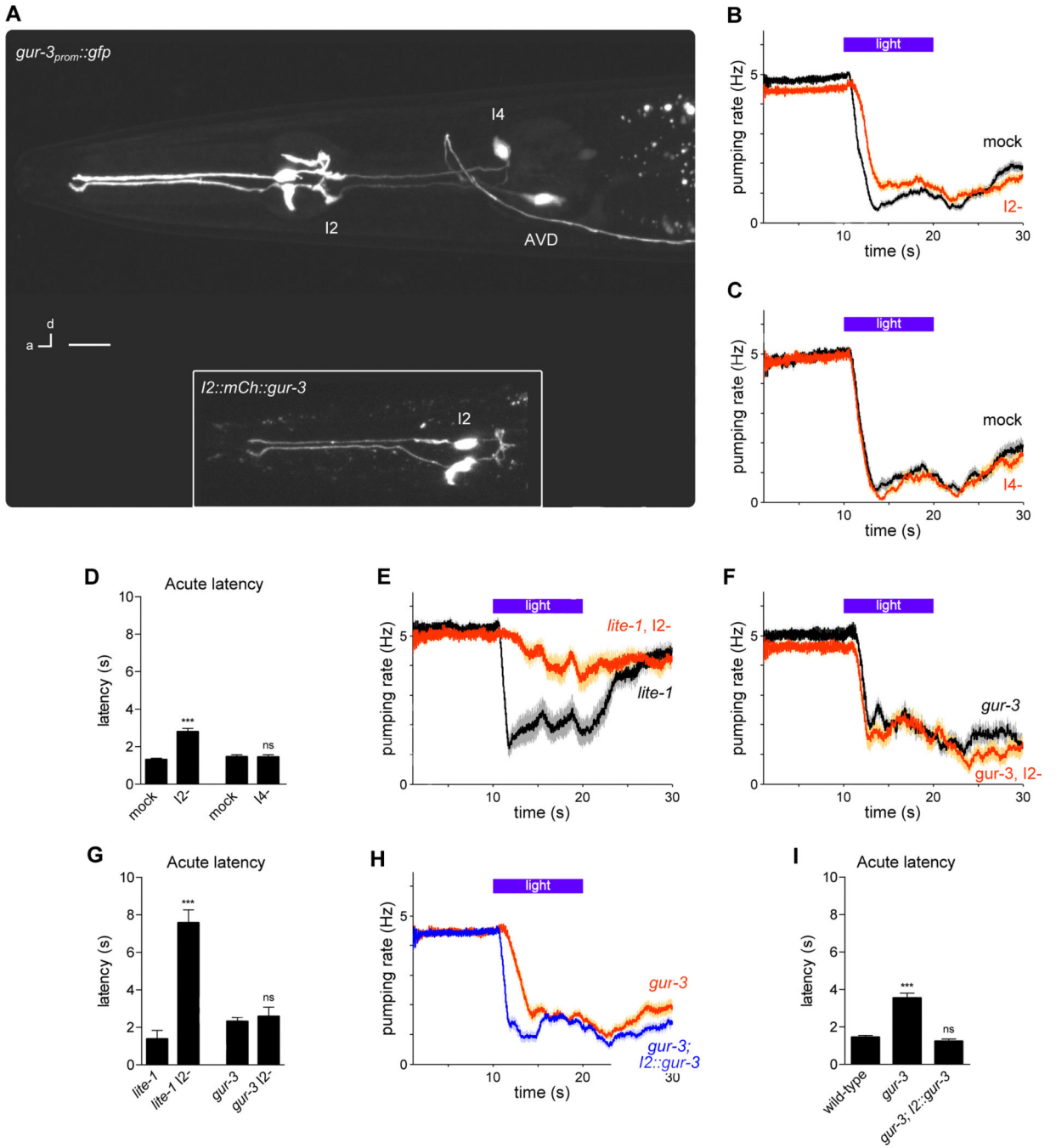


Figure 3. *gur-3* functions in the I2 pharyngeal neurons for light-induced feeding inhibition

(A) *gur-3* was expressed in I2, I4 and AVD, as indicated by a *gur-3_{prom}::gfp* transgene.

Inset: mCherry-tagged *gur-3* was localized throughout I2. Scale bar = 10 μ m.

(B) I2 ablation caused a defect in the acute response to light. n = 32 worms, 72 trials.

(C) I4 ablation did not cause a defect in the pumping response to light. n = 12 worms, 30 trials.

(D) Quantification of acute response latency.

(E) Genetic ablation of I2 in *lite-1* mutants nearly completely abolished the pumping response to light. n = 20 worms.

(F) Genetic ablation of I2 in *gur-3* mutants did not worsen the defect of the pumping response to light of *gur-3* mutants. n = 20 worms.

(G) Quantification of acute response latency.

(H) I2-specific *gur-3* expression restored a normal acute response latency in *gur-3* mutants. n = 60 worms.

(I) Quantification of acute response latency.

Shading around traces and error bars indicate s.e.m. *** $p < 0.001$, ns = not significant, t-test, compared to mock control or wild-type.

See also Figures S1 and S6.

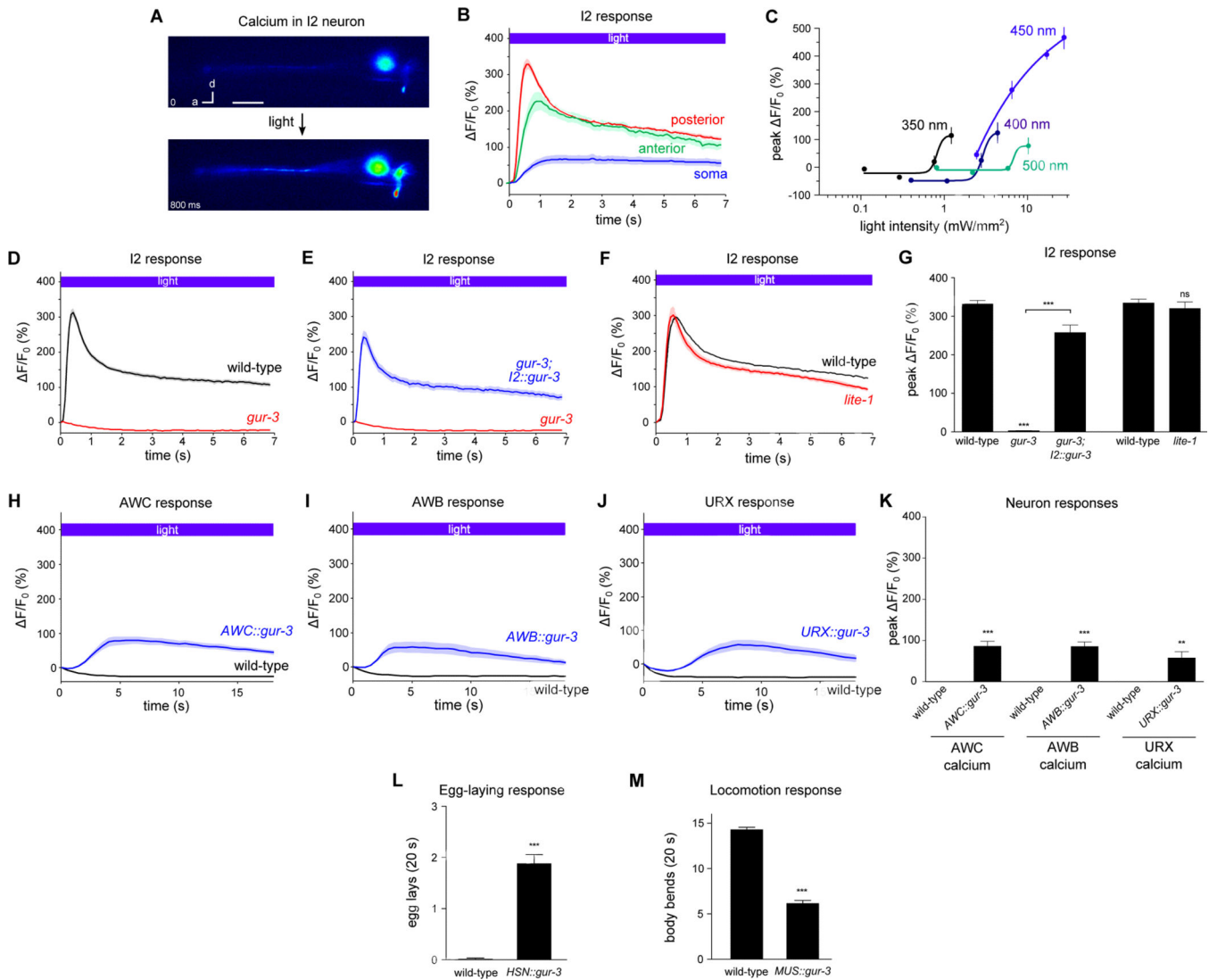


Figure 4. GUR-3 is required for the I2 response to light and is sufficient to confer light-sensitivity to normally light-insensitive neurons and muscle

(A) Representative example of the adult I2 calcium response (GCaMP3) to light (485 nm, 26 mW/mm²). Scale bar = 10 μ m.

(B) Light caused a calcium increase in all three compartments of I2. n = 20 cells.

(C) I2 was most sensitive to shorter wavelengths of light. n = 10 cells per data point.

(D) *gur-3* mutants were completely defective in the I2 response to light. n = 22 cells.

(E) I2-specific *gur-3* expression restored the I2 response to light in *gur-3* mutants. n = 24 cells.

(F) *lite-1* mutants exhibited a normal I2 response to light. n = 20 cells.

(G) Quantification of the peak calcium response in I2 in response to light.

(C-G) The posterior neurite of I2 was analyzed.

(H) AWC-specific *gur-3* expression caused an increase in AWC calcium in response to light, as measured by GCaMP3. n = 16 cells.

(I) AWB-specific *gur-3* expression caused an increase in AWB calcium in response to light, as measured by GCaMP3. n = 11 cells.

(J) URX-specific *gur-3* expression caused a calcium increase in five of 12 URX neurons, as measured by GCaMP. An average of the five responsive neurons is shown.

(K) Quantification of the effect of ectopic *gur-3* expression on somatic neuronal calcium in response to light.

(L) Quantification of the effect of *gur-3* expression in the HSN neurons as measured by egg-laying induced by 20 s of light.

(M) Quantification of the effect of *gur-3* expression in body wall muscle as measured by a reduction in light avoidance during 20 s of light.

Shading around traces and error bars indicate s.e.m. *** $p < 0.001$, t-test or Mann-Whitney test, compared to corresponding wild-type or indicated strain. Transgenes containing “I2” refer to the *flp-15* promoter, “AWC” to the *odr-1* promoter, “AWB” to the *odr-1* promoter, “HSN” to the *egl-6a* promoter, and “MUS” to the *myo-3* promoter. Light for (A, B, D-G) was 485 nm, 26 mW/mm²; light for (H-K) was 485 nm, 10 mW/mm²; and light for (L, M) was 436 nm, 13 mW/mm².

See also Figures S7 and S8 and Movie S2.

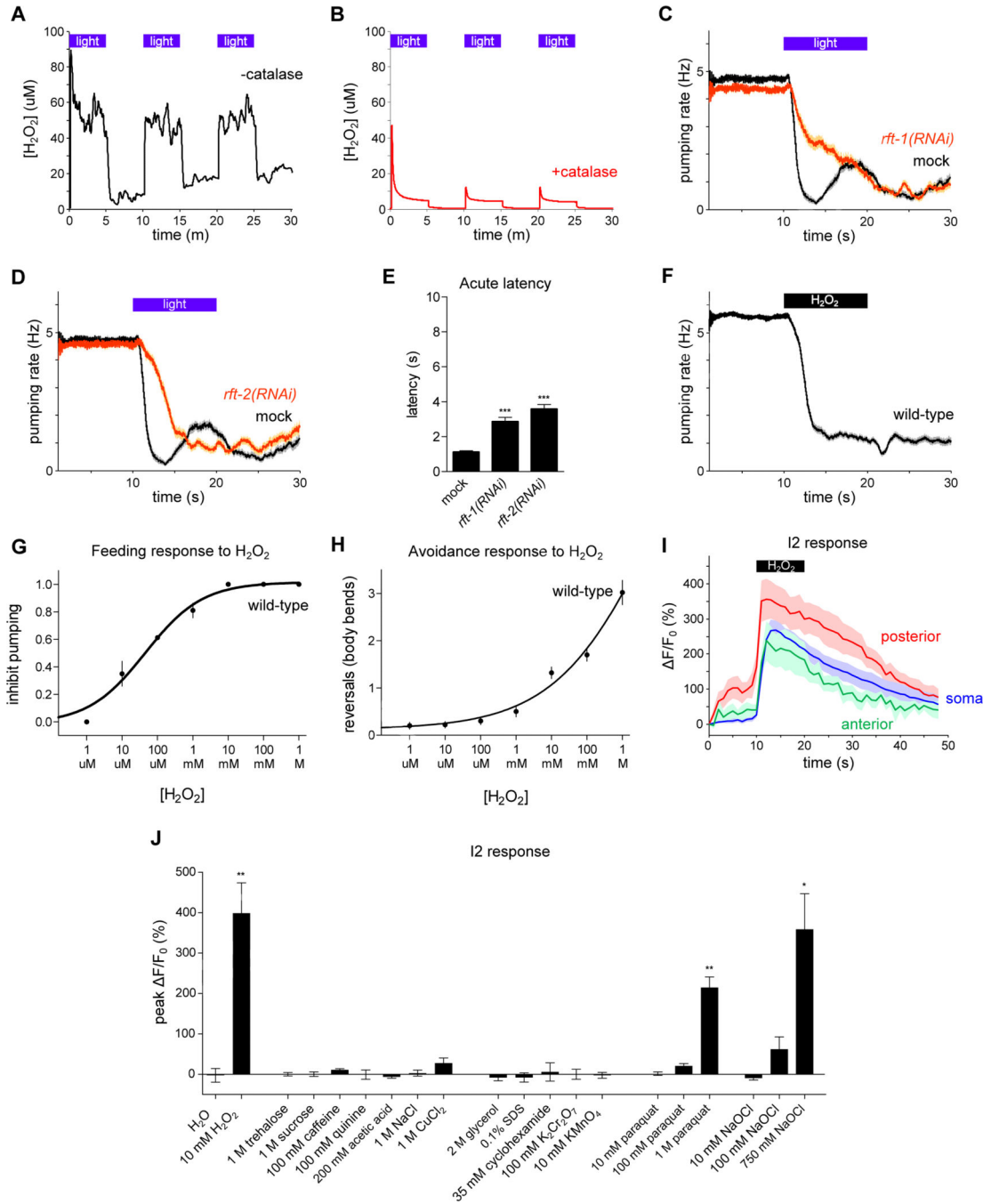


Figure 5. Light can generate hydrogen peroxide and worms respond to hydrogen peroxide.

(A) Light can generate hydrogen peroxide (H₂O₂) in M9 solution containing riboflavin (50 nM) as measured using a hydrogen peroxide sensor electrode. Three pulses of light, identical in power used to expose worms (436 nm, 13 mW/mm²), are shown.

(B) The generation of H₂O₂ by light is reduced in a solution containing catalase (1000 U/ml), indicating that the signal measured by the electrode is in fact hydrogen peroxide. Three pulses of light are shown.

- (C) RNAi against the riboflavin transporter *rft-1* caused a defect in the pumping response to light. n = 60 worms.
- (D) RNAi against the riboflavin transporter *rft-2* caused a defect in the pumping response to light. n = 60 worms.
- (E) Quantification of acute response latency.
- (F) Vapor emitted by H₂O₂ (8.82 M) inhibited feeding by wild-type worms. n = 150 worms.
- (G) Fraction of worms that inhibit pumping in response to various concentrations of liquid H₂O₂. n = 80 worms per data point.
- (H) Number of body bends in a reversal in response to various concentrations of liquid H₂O₂. n = 40 worms per data point.
- (I) All three compartments of the I2 neurons responded to H₂O₂ vapor (8.82 M). n = 10 cells.
- (J) Quantification of the I2 calcium response to a panel of compounds dissolved in water. Hydrogen peroxide (10 mM), paraquat (1 M) and sodium hypochlorite (750 mM) activated the I2 neuron, while all other compounds failed to elicit an effect. n = 3 cells. Shading around traces and error bars indicate s.e.m. * p < 0.05, ** p < 0.01, *** p < 0.001, t-test compared to mock control or water control. See also Figure S9.

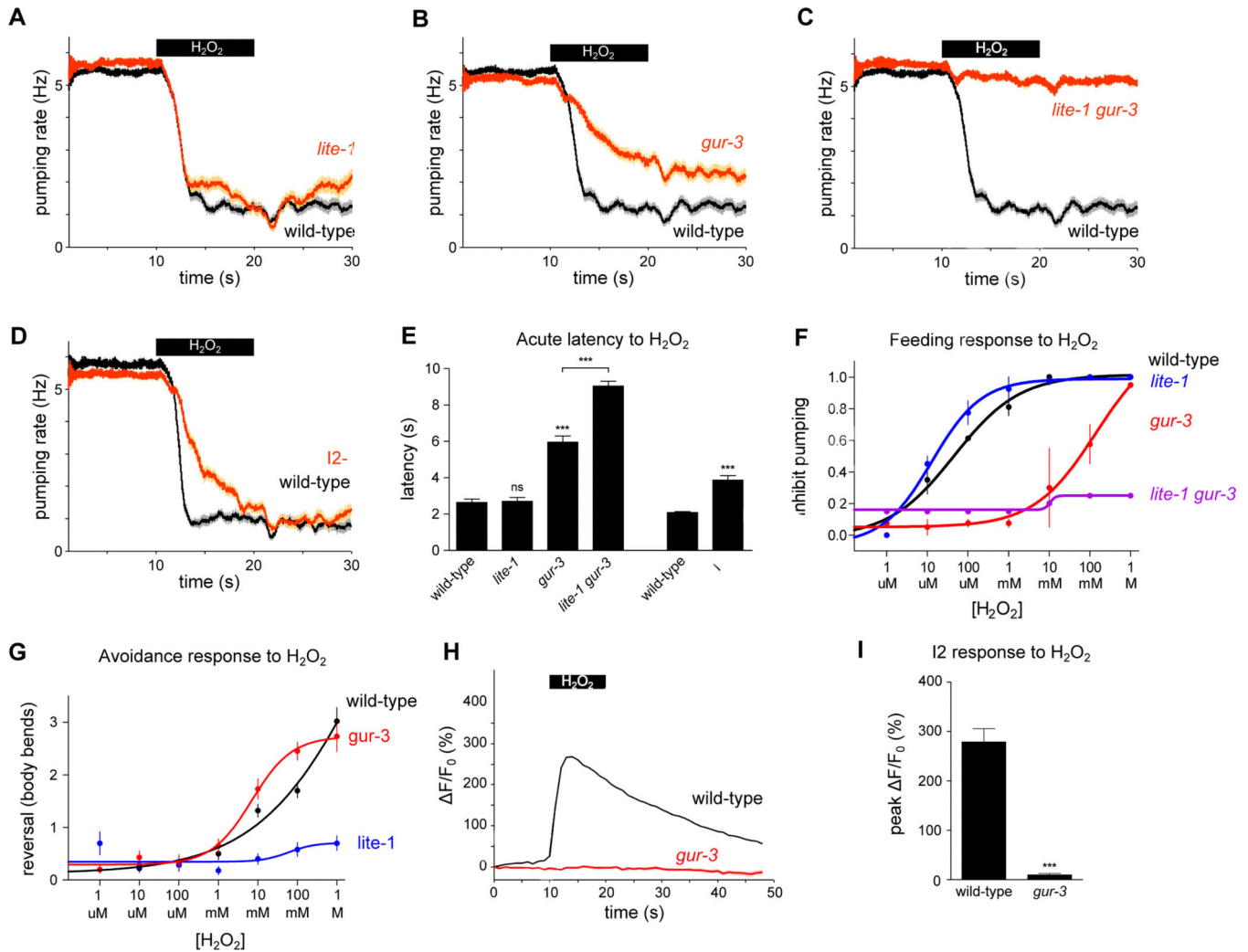


Figure 6. Responses to hydrogen peroxide require *gur-3* and *lite-1*

(A) *lite-1* mutants inhibited pumping in response to H₂O₂ vapor like wild-type worms. n = 64 worms.

(B) *gur-3* mutants exhibited a defect in the pumping response to H₂O₂ vapor. n = 78 worms.

(C) *lite-1 gur-3* double mutants were nearly completely defective in the pumping response to H₂O₂ vapor. n = 72 worms.

(D) Genetic ablation of the I2 neurons resulted in a defect in response to H₂O₂ vapor. n = 60 worms.

(E) Quantification of the acute response latency to H₂O₂ vapor.

(F) Fraction of worms that inhibit pumping in response to various concentrations of liquid H₂O₂. *lite-1* mutants responded normally across a range of H₂O₂ concentrations. *gur-3* mutants showed a reduced sensitivity to H₂O₂, and *lite-1 gur-3* double mutants were completely defective in the pumping response to H₂O₂. *lite-1 gur-3* data points do not have error bars because only one experiment was done. n = 20 worms per data point.

(G) Number of body bends in a reversal in response to various concentrations of liquid H₂O₂. *lite-1* mutants were completely defective in avoiding H₂O₂, while *gur-3* mutants were not defective. n = 20 worms per data point.

(H) The I2 neurons failed to respond to H₂O₂ vapor in *gur-3* mutants. The response in the I2 soma is shown; all three compartments failed to respond in *gur-3* mutants (other compartments not shown). n = 10 cells.

(I) Quantification of the I2 calcium response to H₂O₂ vapor.

Shading around traces and error bars indicate s.e.m. *** p < 0.001, ns = not significant, t-test compared to corresponding wild-type or indicated strain.

See also Figure S10.

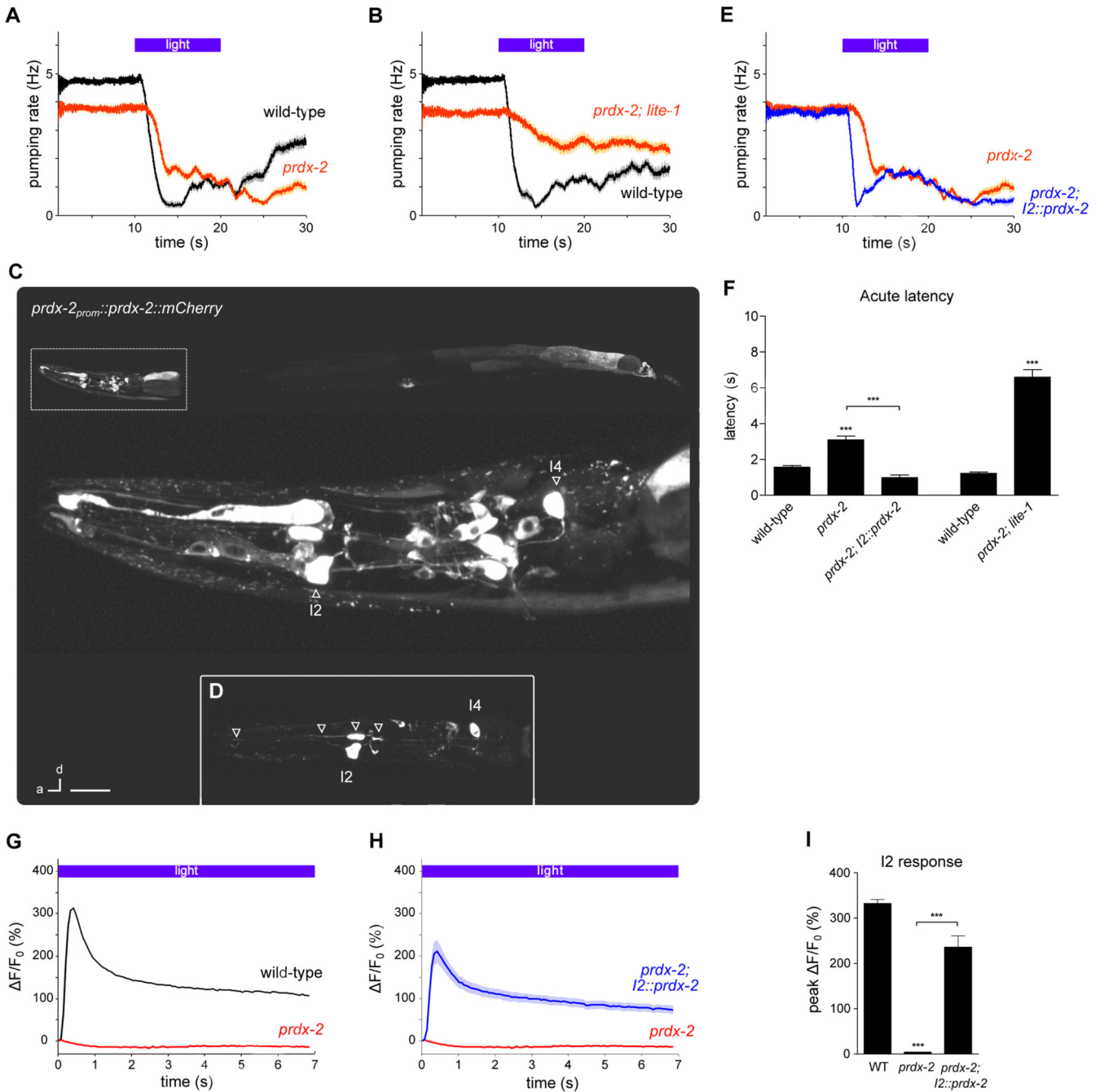


Figure 7. The peroxiredoxin *prdx-2* functions in the I2 neurons for feeding inhibition by light
 (A) *prdx-2(gk169)* mutants had a defective acute response to light. n = 60 worms.
 (B) *prdx-2; lite-1* double mutants had a worse defect than *prdx-2* single mutants. n = 60 worms.
 (C) *prdx-2* showed a broad expression pattern, as indicated by a functional *prdx-2_{promi}::prdx-2::mCherry* transgene with mosaic transmission.

(D) Inset: mCherry-tagged *prdx-2* was localized throughout I2. Arrowheads point to two parts of the anterior neurite, the soma, and the posterior neurite. Scale bar = 50 μm (top), 10 μm (middle), 20 μm (inset).

(E) I2-specific *prdx-2* expression restored a normal pumping response in *prdx-2* mutants. $n = 60$ worms.

(F) Quantification of the acute response latency to light.

(G) *prdx-2* mutants were completely defective in the I2 response to light. $n = 20$ cells.

(H) I2-specific *prdx-2* expression restored the I2 response to light in *prdx-2* mutants. $n = 20$ cells.

(I) Quantification of the peak response of the I2 neurons to light.

(G-I) The posterior neurite of I2 was analyzed.

Shading around traces and error bars indicate s.e.m. *** $p < 0.001$, t-test compared to the corresponding wild-type or indicated strain.

See also Figures S7 and S11.

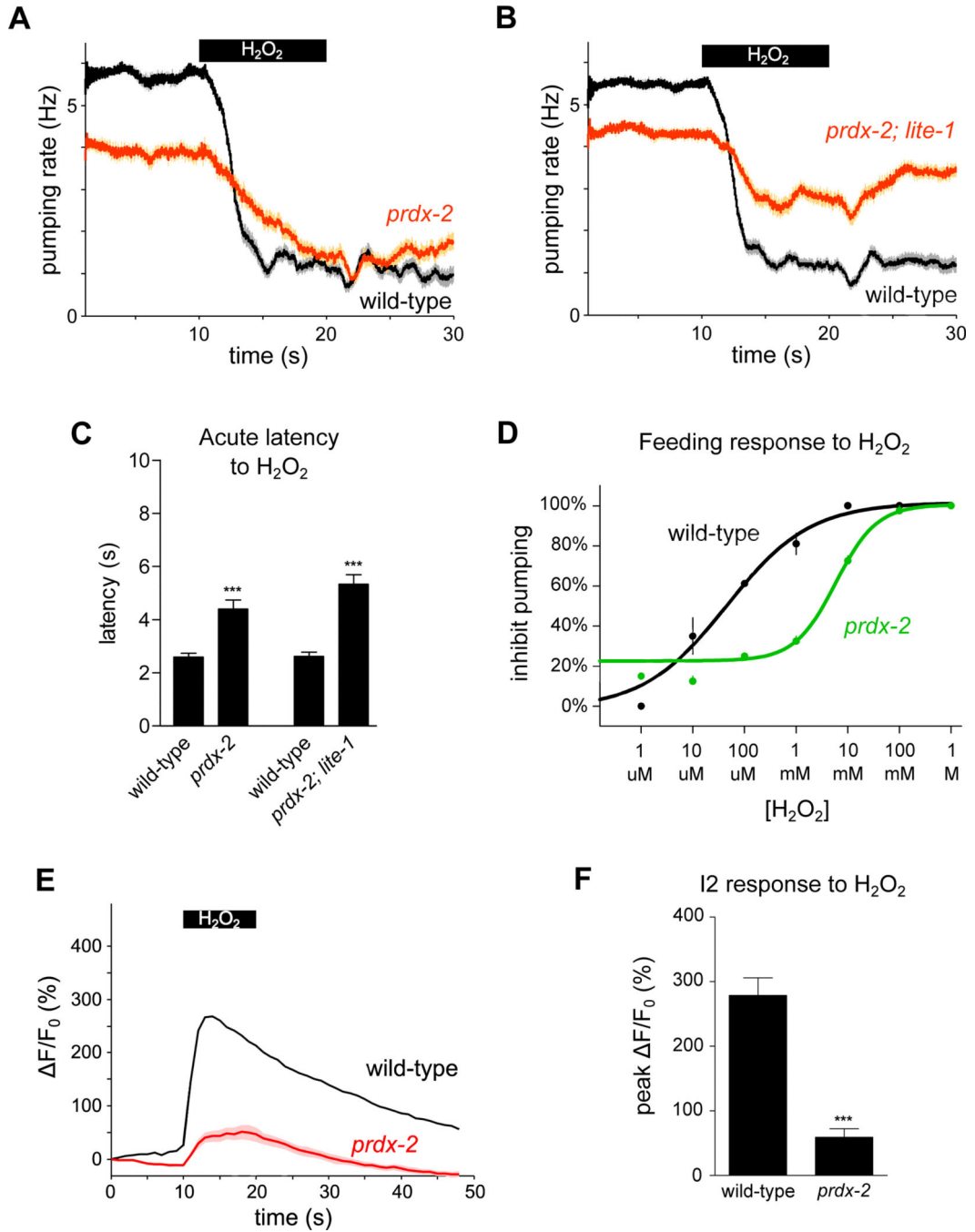


Figure 8. *prdx-2* is required for feeding inhibition and the I2 calcium response caused by hydrogen peroxide

- (A) *prdx-2* mutants were defective in the acute response to H₂O₂ vapor. n = 60 worms.
- (B) *prdx-2; lite-1* double mutants were more defective in the pumping response to H₂O₂ than *prdx-2* mutants. n = 86 worms.
- (C) Quantification of the acute response latency to H₂O₂ vapor.
- (D) *prdx-2* mutants were defective in the pumping response to H₂O₂ liquid.
- (E) *prdx-2* mutants were defective in the I2 soma response to H₂O₂ vapor.

(F) Quantification of the peak response of the I2 neurons to H₂O₂ vapor. Shading around traces and error bars indicate s.e.m. *** p < 0.001, t-test.

Author Manuscript

Author Manuscript

Author Manuscript

Author Manuscript